

THREE-DIMENSIONAL WAVES GENERATED AT LINDBLAD RESONANCES IN THERMALLY STRATIFIED DISKS

S. H. LUBOW AND G. I. OGILVIE¹
 SPACE TELESCOPE SCIENCE INSTITUTE
 3700 SAN MARTIN DRIVE
 BALTIMORE, MD 21218

Accepted for publication in the Astrophysical Journal

ABSTRACT

We analyze the linear, 3D response to tidal forcing of a disk that is thin and thermally stratified in the direction normal to the disk plane. We model the vertical disk structure locally as a polytrope which represents a disk of high optical depth. We solve the 3D gas-dynamic equations semi-analytically in the neighborhood of a Lindblad resonance. These solutions match asymptotically on to those valid away from resonances (previously obtained by Korycansky & Pringle 1995) and provide solutions valid at all radii r . We obtain the following results. 1) A variety of waves are launched at resonance, including r modes and g modes. However, the f mode carries more than 95% of the torque exerted at the resonance. 2) These 3D waves collectively transport exactly the amount of angular momentum predicted by the standard 2D resonant torque formula. 3) Near resonance, the f mode behaves compressibly and occupies the full vertical extent of the disk. Away from resonance, the f mode behaves incompressibly, becomes confined near the surface of the disk, and, in the absence of other dissipation mechanisms, damps via shocks. In general, the radial length scale for this process is roughly r_L/m (for resonant radius r_L and azimuthal tidal forcing wavenumber m), *independent of the disk thickness H* . This wave channeling process is due to the variations of physical quantities in r and is not due to wave refraction. 4) However, the inwardly propagating f mode launched from an $m = 2$ inner Lindblad resonance experiences relatively minor channeling (accompanied by about a factor of 5 increase in nonlinearity), all the way to the radial center of the disk.

We conclude that for binary stars, tidally generated waves at Lindblad resonances in highly optically thick circumbinary disks are subject to strong nonlinear damping by the channeling mechanism, while those in circumstellar accretion disks are subject to weaker nonlinear effects. We also apply our results to waves excited by young planets for which $m \approx r/H$ and conclude that the waves are damped on the scale of a few H .

Subject headings: accretion: accretion disks — binaries: close — planetary systems — solar system: formation — stars: pre-main-sequence

1. INTRODUCTION

Gaseous disks are found in many types of binary star systems, including cataclysmic variables (CVs) and pre-main-sequence stars, and young planetary systems. The orbiting objects (stars or planets) exert tidal forces on these disks, which generally act merely to distort the disks from an axisymmetric form. However, at special locations in disks where resonances occur, the tidal forces generate waves that transport energy and angular momentum. As a result, a resonant torque is exerted by the system objects. The orbital evolution of the perturbing objects sometimes depends on the strength of these torques (Goldreich & Tremaine 1980, hereafter GT80; Lin & Papaloizou 1993; Lubow & Artymowicz 1996). The waves transfer their angular momentum and energy to the disk in the regions of space where they damp, and this in turn affects the evolution of the disk. For example, gaps could be created in disks in regions where the waves damp.

This paper concentrates on Lindblad resonances (LRs), which are due to horizontal forcing (along the disk plane). We assume throughout that the disk is coplanar with the orbit of the system objects. A 2D, linear theory for

resonant tidal torques and associated wave propagation was developed by Goldreich & Tremaine (1979, hereafter GT79). This theory provides an explicit formula for the Lindblad resonant torque. The 2D theory considers the disk to have only radial and azimuthal extent and ignores effects over its vertical extent (perpendicular to the orbit plane). Important progress has been made in the study of 2D nonlinear waves in disks (Shu, Yuan, & Lissauer 1985; Yuan & Cassen 1994). The torque in the nonlinear case was found to be within a few percent of that predicted by the 2D linear formula. The nonlinearities produce highly spiked density profiles which increase the level of dissipation present in a viscous disk. Radiative damping of linear waves can be important particularly when the disk is warm (Cassen & Woolum 1996). Turbulent viscosity in the disk provides another means of wave damping.

The 2D treatment is valid if both the vertical structure of the disk and its thermodynamic response are locally isothermal. Under such circumstances, tidal forcing will generate a 2D wave in a 3D disk. The wave front remains perpendicular to the disk plane at all heights, as the wave propagates radially in the disk. However, this 2D wave is highly singular in that it does not exist in a disk with a ver-

¹Present address: Institute of Astronomy, University of Cambridge, Madingley Road, Cambridge CB3 0HA, United Kingdom.

tical temperature variation (Lin, Papaloizou, & Savonije 1990a, hereafter LPS; Lubow & Pringle 1993, hereafter LP). Furthermore, a vertically isothermal structure is not realistic for many important classes of gaseous disks, such as accretion disks in CVs, circumstellar and circumbinary disks of YSOs, and protoplanetary disks. Such disks often have optical depths much greater than unity and can be expected to have substantial vertical temperature variations, if they have an internal heat source such as turbulent dissipation.

We demonstrate in this paper that 2D tidal forcing, caused by LRs, excites 3D waves in a thermally stratified disk. However, another class of resonances exist due to 3D effects. These resonances are due to vertical, tidal forcing by a coplanar perturber of a disk with nonzero thickness (Lubow 1981). The vertical resonances also generate horizontally propagating waves. Although intrinsically weaker than the LRs, the vertical resonances may be of importance in close binary star systems.

Some investigations of 3D effects have been carried out using numerical simulations (Lin, Papaloizou, & Savonije 1990a,b). Such approaches can be used to explore a limited range of physical parameter space. However, recent progress has been made in obtaining semi-analytic solutions for waves in 3D disks (LP; Korycansky & Pringle 1995, hereafter KP). The aim of this paper is to extend that approach to understand 3D wave generation at LRs and the subsequent wave propagation. We determine the linear response of a thin (but nonzero thickness) disk. We model the disk locally as a polytrope in the vertical direction, which is valid for a disk of very high optical depth, and we ignore the effects of atmospheric layers. We aim to understand which modes of a thermally stratified disk are excited at LRs and how much torque is carried by such waves. By studying the properties of linear wave propagation, we can also understand where nonlinearity sets in that will likely lead to shocks and subsequent wave dissipation.

The outline of this paper is as follows. In §2, we review the properties of disk modes. In §3 and §4, we derive and solve the equations for waves generated at LRs. In §5, we compute the total torque carried by these waves and determine which modes are excited. In §6, we summarize properties of the f mode of the disk and present our numerical results. In §7, we discuss the application of our results to binary and protoplanetary systems. §8 contains a summary.

2. REVIEW OF THREE-DIMENSIONAL WAVES IN A THIN DISK

2.1. *Free Waves*

In a thin disk, there is a separation of scales between the horizontal and vertical directions which implies that the waves take a WKB form in the radial direction, except in the neighborhood of resonances, which are also turning points for the waves. The equations governing axisymmetric WKB waves in a vertically isothermal disk are described in LP within the approximation of the shearing sheet, in which the radial derivatives of all base-state quantities other than the angular velocity are neglected. The case of a vertically polytropic disk was subsequently considered by KP.

The problem reduces to a second-order system of ordinary differential equations in the vertical coordinate z , which, together with appropriate boundary conditions, constitutes an eigenvalue problem for the frequency ω of the mode. The radial wavenumber $k(r)$ appears as a parameter, so that a local dispersion relation $\omega(k; r)$ is defined. Moreover, the same dispersion relation applies to non-axisymmetric waves if the frequency eigenvalue ω is replaced by the intrinsic frequency $\hat{\omega} = \omega - m\Omega$, provided that the azimuthal wavenumber $m > 0$ satisfies $m \ll r/H$.

The solutions of the eigenvalue problem can be classified by analogy with the theory of stellar oscillations (e.g. Cox 1980). The name of each class of mode refers to the dominant restoring force that is involved in its dynamics. Thus p modes are acoustic modes, which are inherently compressible and propagate by pressure forces. The g modes are gravity modes, which rely on buoyancy forces resulting from an entropy gradient in the vertical direction. There are also r modes, which do not exist in a non-rotating star, and which propagate by inertial forces. The p, g, and r modes can be further classified according to their symmetry about the mid-plane and the number of nodes in the pressure perturbation (or radial velocity perturbation) in $z > 0$. Finally, the f mode is the fundamental mode of oscillation, and has unique characteristics described in detail in §6.1 below. In fact, a disk has two f modes, one of each symmetry, because it has two surfaces.

Some of these modes are lost in special cases. In an incompressible disk, there are no p modes, although all other modes survive. The g modes do not exist in a disk that is adiabatically stratified in the vertical direction. Similarly, there are no r modes in a disk that has zero epicyclic frequency. In an isothermal disk with no surface, the g modes are lost and the f mode of even symmetry takes a special form, known otherwise as the Lamb mode or two-dimensional mode. (There has been some confusion in terminology. LP used the naming convention that r modes were called g modes.)

For a monochromatic wave or a normal mode of the disk, ω is independent of r and the dispersion relation can be followed continuously to determine the wavenumber at any radius. Typically, the wave occupies a finite interval in radius, which is bounded either by turning points, at which k goes to zero, or by the edges of the disk. Moreover, the continuous variation of the amplitude of the wave with r can be determined by appealing to the conservation of either energy or angular momentum wave action.

In many cases of interest, the dispersion relation is followed into a limit in which the dimensionless wavenumber kH becomes large. The behavior of the modes in this limit was described by Ogilvie (1998). Provided that the disk has a surface, the f, p, and g modes become confined in a layer of characteristic thickness k^{-1} near the surface, and their frequencies scale proportionally to $k^{1/2}$. In contrast, the r modes become confined in a layer of characteristic thickness $k^{-1/2}H^{1/2}$ centered on the mid-plane, and their frequencies scale proportionally to $k^{-1/2}$, unless the disk is marginally stable to convection. None of the modes occupies the full vertical extent of the disk in this limit.

It is useful to note the following properties of waves in a Keplerian disk. The f and g modes have $|\hat{\omega}| \geq \Omega$ and propagate both inside the inner LR and outside the outer LR. The r modes have $|\hat{\omega}| \leq \Omega$ and propagate in the re-

gion between the two LRs, where the corotation resonance is also located. An exception is the ‘tilt’ mode, consisting of the union of the f and r_1 modes of odd symmetry, which propagates at all radii. The p modes have $|\hat{\omega}| \geq \omega_p$, where $\omega_p > \Omega$ is a frequency which increases with the order of the mode. Their resonances are separated from the Lindblad resonances by a distance which also increases with the order of the mode. These properties are summarized in Figure 1.

2.2. Asymptotic Matching

One of the goals of this paper is to determine to level of excitation of the free modes described above, due to tidal forcing at Lindblad resonances. To accomplish this, we determine in §4 the solutions for the tidally generated waves in a small region close to the Lindblad resonance (of order $(H^2 r)^{1/3}$ in radius), where the wave excitation occurs. In this region of space, a locally valid approximation is used, in which the quantity $\kappa^2 - \hat{\omega}^2$, which has a zero at the resonance, is treated as a linear function of radius. Away from the resonance (over most of space), a different approximation applies, which is a WKB approximation in the radial direction. Radial WKB free wave solutions of a vertically polytropic disk were obtained by KP. A solution that is uniformly valid for all r (asymptotically accurate in all space in the limit $H \ll r$) is obtained by the method of matched asymptotic expansions (e.g. van Dyke 1975). In this context, the global wave solutions are determined by matching the outer limit (limit going away from resonance) of the driven Lindblad resonance solutions to the inner limit (limit approaching resonance) of the KP free waves. In practice, the level of excitation of each KP mode is easily determined from the amount of angular momentum generated for that mode in the region near resonance.

3. MATHEMATICAL FORMULATION

3.1. Base state

Consider a cylindrical coordinate system (r, ϕ, z) such that $z = 0$ coincides with the disk mid-plane and the direction of increasing ϕ is the direction of disk rotation. The unperturbed disk has angular velocity $\Omega(r)$, density $\rho(r, z)$, and pressure $p(r, z)$. We assume that the disk is thin and ignore effects of viscosity and self-gravity. As in KP, we adopt a polytropic disk structure in z locally in r so that

$$\rho(r, z) = \rho_0(r)(1 - z^2/H^2)^s \quad (1)$$

and

$$p(r, z) = p_0(r)(1 - z^2/H^2)^{s+1}, \quad (2)$$

where $\rho_0(r)$ and $p_0(r)$ are arbitrary smooth functions of r and s is the polytropic index. The disk half-thickness $H(r)$ satisfies

$$H^2(r) = \frac{2(s+1)p_0(r)}{\Omega^2(r)\rho_0(r)}. \quad (3)$$

The thin-disk approximation used to derive the above requires $H \ll r$. The base-state angular velocity is slightly modified from a Keplerian law by the radial pressure forces and it varies slightly in z within the disk. However, these effects are unimportant for the issues described in this

paper and are generally ignored. The polytropic structure provides a mathematically convenient description of a thermally stratified disk of high optical depth. However, the features of the results obtained in subsequent sections do not depend on the thermally stratified disk being polytropic.

3.2. Dynamical equations

Let the local Eulerian perturbations of disk velocity in cylindrical coordinates be represented by (u, v, w) , that of pressure by p' , and that of density by ρ' . We represent physical wave quantities such as the pressure perturbation by $p'(r, \phi, z, t) = p'(r, z) \exp[i m(\phi - \Omega_p t)]$, where positive integer m is the azimuthal wavenumber and Ω_p is the angular pattern speed of the wave. Consider the disk to be subject to a tidal potential component $\Phi_m(r, \phi, z, t)$ of the above form. In the case that the system objects are in circular orbits, the pattern speed is equal to the angular orbital speed of the objects. If the system has eccentricity, then additional components of the perturbing potential appear containing the pattern speeds that differ from the fundamental orbital frequency of the system (see GT80). Using the 3D shearing sheet equations (see LP and KP), we obtain the following equations for the disk perturbations.

$$-i\hat{\omega}u - 2\Omega v + \frac{\partial_r p'}{\rho} = -\frac{d\Phi_m}{dr}, \quad (4)$$

$$-i\hat{\omega}v + 2Bu = -\frac{im}{r}\Phi_m, \quad (5)$$

$$-i\hat{\omega}w + g\frac{\rho'}{\rho} + \frac{\partial_z p'}{\rho} = 0, \quad (6)$$

$$-i\hat{\omega}\frac{\rho'}{\rho} + w\partial_z \ln \rho + \partial_r u + \partial_z w = 0, \quad (7)$$

and

$$-i\hat{\omega}\left(\frac{p'}{p} - \gamma\frac{\rho'}{\rho}\right) + w\partial_z \ln\left(\frac{p}{\rho^\gamma}\right) = 0, \quad (8)$$

where γ is the usual adiabatic exponent. These equations are respectively the radial, azimuthal, and vertical force equations, the mass conservation equation, and the energy equation for adiabatic perturbations. The frequency $\hat{\omega}$ is defined as

$$\hat{\omega}(r) = m[\Omega_p - \Omega(r)]. \quad (9)$$

Quantity $B(r)$ is the usual Oort constant equal to $\Omega + \frac{r}{2}\frac{d\Omega}{dr}$ and g is the vertical gravity in the disk equal to $g(r, z) = \Omega^2(r)z$. The azimuthal pressure force imp'/r was ignored in equation (5) and the azimuthal velocity term imv/r was ignored in equation (7). This approximation is justified for a thin-disk limit for which

$$H \ll r/m. \quad (10)$$

The forcing term in the vertical force equation (6) was ignored. This approximation can be justified by the thin-disk condition (10) everywhere except at vertical resonance points (Lubow 1981). We concentrate on wave properties near Lindblad resonances (horizontal resonances) in this paper and thus this approximation is justified.

4. EQUATIONS NEAR LRS

By combining equations (4) and (5), we obtain

$$u(\hat{\omega}^2 - \kappa^2) + i\hat{\omega} \frac{\partial_r p'}{\rho} = -i\hat{\omega} \frac{d\Phi_m}{dr} + \frac{2im\Omega}{r} \Phi_m, \quad (11)$$

where κ is the epicyclic frequency such that $\kappa^2 = 4B\Omega$. Notice that equations (6)–(8), together with equation (11), form a complete set, i.e., v has been eliminated. Once u has been determined, v can be obtained from equation (5).

LRs occur at radii r_L where $\hat{\omega}^2 = \kappa^2$. Away from such locations, the above equations are equivalent to the WKB equations of KP. Near an LR, the WKB approximation breaks down in equation (11), but the solutions can be represented in terms of Airy functions in the neighborhood of the turning point. To treat this region, we follow standard techniques (e.g. GT79) and expand in the neighborhood of the resonance

$$\kappa^2 - \hat{\omega}^2 \approx \mathcal{D}x, \quad (12)$$

where $x = (r - r_L)/r_L$, and $\mathcal{D} = rd(\kappa^2 - \hat{\omega}^2)/dr$ is evaluated at $r = r_L$. We then approximate the radial force equation by

$$-u\mathcal{D}x + i\hat{\omega} \frac{\partial_r p'}{\rho} = -i\hat{\omega} \frac{d\Phi_m}{dr} + \frac{2im\Omega}{r} \Phi_m. \quad (13)$$

4.1. Free waves

The equations for free waves near LRs are obtained by setting $\Phi_m = 0$ and combining equations (6)–(8) and (13). We seek solutions of the following form.

$$\begin{aligned} u(x, z) &= Ai(qx)\tilde{u}(z), \\ v(x, z) &= iAi(qx)\tilde{v}(z), \\ w(x, z) &= qAi'(qx)\tilde{w}(z), \\ p'(x, z) &= iqAi'(qx)\tilde{p}'(z), \\ p(x, z) &= iqAi'(qx)\tilde{p}(z), \end{aligned} \quad (14)$$

where Ai is the Airy function given by equation (10.4.1) of Abramowitz & Stegun (1965) and Ai' is the derivative with respect to its argument. The parameter q is a dimensionless constant that will be determined as an eigenvalue. (Solutions involving the complementary Airy function Bi have been discarded because, on one side of resonance, they approach infinity with distance from the resonance.)

Using the property that $Ai''(x) = xAi(x)$, we obtain the following free-wave equations for $\tilde{u}, \tilde{v}, \tilde{w}, \tilde{p}'$ and \tilde{p}' .

$$\rho\mathcal{D}\tilde{u} + \frac{\hat{\omega}q^3}{r}\tilde{p}' = 0, \quad (15)$$

$$\tilde{v} = -\frac{2B}{\hat{\omega}}\tilde{u}, \quad (16)$$

$$\hat{\omega}\rho\tilde{w} - g\tilde{p}' - \frac{d\tilde{p}'}{dz} = 0, \quad (17)$$

$$\hat{\omega}\tilde{p}' + \tilde{w}\frac{d\rho}{dz} + \rho\left(\frac{\tilde{u}}{r} + \frac{d\tilde{w}}{dz}\right) = 0, \quad (18)$$

and

$$\hat{\omega}\left(\frac{\tilde{p}'}{p} - \gamma\frac{\tilde{p}'}{\rho}\right) + w\frac{d}{dz}\ln\left(\frac{p}{\rho^\gamma}\right) = 0, \quad (19)$$

where all coefficients are evaluated at $r = r_L$.

As can be seen from the above, the equations have been reduced to 1D equations in z . We introduce dimensionless variables

$$\begin{aligned} Z &= z/H, \\ X(Z) &= \hat{\omega}\tilde{p}'(z)/(\Omega^3 H^2 \rho), \\ F &= \hat{\omega}/\Omega, \\ Q &= (H/r)^{2/3}q, \\ S &= \mathcal{D}/\Omega^2, \\ W(Z) &= \tilde{w}(z)/(\Omega H). \end{aligned} \quad (20)$$

Combining the above equations (15)–(20), we obtain

$$\frac{dX}{dZ} - \left(\frac{2\alpha Z}{1 - Z^2}\right) X - \left(F^2 - \frac{2\alpha Z^2}{1 - Z^2}\right) W = 0 \quad (21)$$

and

$$\frac{dW}{dZ} - \left(\frac{2\beta Z}{1 - Z^2}\right) W + \left(\frac{2\beta}{1 - Z^2} - \frac{Q^3}{S}\right) X = 0, \quad (22)$$

where the constants $\alpha = s - (1 + s)/\gamma$ and $\beta = (1 + s)/\gamma$ are proportional to the square of the disk's buoyancy frequency and the square of the inverse sound speed at mid-plane, respectively. We note that these equations can be derived from equations (13) and (14) of KP in an expansion about the point of the dispersion relation where $k = 0$ and $F^2 = \kappa^2$.

Equations (21) and (22) are integrated numerically with appropriate boundary conditions at $Z = 0$ and $Z = 1$, as in KP. Both even and odd solutions about $Z = 0$ can be obtained, but for the coplanar forcing problem at hand, only even solutions are relevant. Such solutions must then satisfy $W(0) = 0$. Infinitely many solutions exist which differ in n , the number of vertical nodes of X (the pressure perturbation) for $Z > 0$. At $Z = 1$, the boundary condition is that the Lagrangian pressure perturbation must vanish. Solutions are obtained by numerically integrating out of the regular singular point $Z = 1$ down to $Z = 0$. Only certain values of Q permit the mid-plane boundary condition $W = 0$ to be satisfied. Once the value of Q is determined, the spatial structure of all physical quantities is known. Solutions with various spatial structures are obtained that behave as g modes, r modes, and the f mode. Each solution is characterized by the type of mode (g, r, etc.) and by the value of n . There are a countably infinite number of solutions, which we label by index j .

We note that the scalings for a thin disk are such that q is of order $(r/H)^{2/3}$. The characteristic width of the resonance is therefore $(H^2 r)^{1/3}$, intermediate between H and r . In addition, the vertical component of the velocity is smaller than the horizontal components by a factor of order $(H/r)^{1/3}$.

4.2. Driven waves

We return to the problem of wave generation due to tidal forcing. We consider solutions to the inhomogeneous equations near resonance, equations (6)–(8) and (13). We consider the set of all homogeneous solutions obtained in the last section, each of which is characterized by the set of physical quantities $q_j, \tilde{u}_j(z), \tilde{v}_j(z), \tilde{w}_j(z), \tilde{p}'_j(z)$, and

$\tilde{p}'_j(z)$. We construct possible solutions to the inhomogeneous equations which are expanded in terms of the homogeneous solutions in the following way.

$$\begin{aligned} u(x, z) &= \sum_j a_j \tilde{u}_j(z) [Ai(q_j x) + is_j Gi(q_j x)], \\ w(x, z) &= \sum_j a_j q_j \tilde{w}_j(z) [Ai'(q_j x) + is_j Gi'(q_j x)], \\ p'(x, z) &= i \sum_j a_j q_j \tilde{p}'_j(z) [Ai'(q_j x) + is_j Gi'(q_j x)], \\ p'(x, z) &= i \sum_j a_j q_j \tilde{p}'_j(z) [Ai'(q_j x) + is_j Gi'(q_j x)], \end{aligned} \quad (23)$$

where Gi is the inhomogeneous Airy function defined in equation (10.4.55) of Abramowitz & Stegun (1965), s_j is either $+1$ or -1 , and a_j are the expansion coefficients. The linear combination of Airy functions, $Ai(q_j x) + is_j Gi(q_j x)$ and $Ai'(q_j x) + is_j Gi'$, in the above is chosen to provide traveling waves in the limit $q_j x \rightarrow -\infty$. The sign of s_j in the above determines the radial propagation direction of the wave (toward or away from the resonance) which we leave as an open issue for now for each j .

We use the fact that Gi satisfies $Gi''(x) - xGi(x) = -1/\pi$, and substitute the above forms into inhomogeneous equations (6)–(8) and (13). We find that equations (6)–(8) are automatically satisfied and do not in any way constrain the expansion coefficients. The constraint comes from the force equation (13), which is satisfied provided that

$$\Psi_m = -\frac{1}{\pi} \sum_j s_j a_j q_j^2 \frac{\tilde{p}'_j(z)}{\rho(z)}, \quad (24)$$

where forcing term Ψ_m is defined by

$$\Psi_m = r \frac{d\Phi_m}{dr} - \frac{2m\Omega}{\hat{\omega}} \Phi_m, \quad (25)$$

evaluated at $r = r_L$. In equation (24), the left-hand side is independent of z . In the case of an isothermal disk with adiabatic index equal to unity ($\gamma = 1$), the ratio \tilde{p}'_j/ρ is independent of z (and proportional to the sound speed squared) for the 2D mode, which is then the proper solution in that case only. In general, for disks with non-isothermal vertical structures or vertically isothermal disks having $\gamma \neq 1$, the quantity \tilde{p}'_j/ρ varies with z for all modes in the disk. So some suitable combination of solutions is required.

To solve equation (24), we seek an appropriate inner product that allows us to invert that equation to solve for a_j . This can be derived by noting that equations (15)–(19) can be combined to give a single equation for \tilde{u} in the form

$$\frac{d}{dz} \left(f_1 \frac{d\tilde{u}}{dz} \right) + f_2 \tilde{u} + \frac{\lambda \rho \tilde{u}}{H^2 \Omega^2} = 0, \quad (26)$$

where

$$f_1 = \frac{\rho}{N^2 - \hat{\omega}^2}, \quad (27)$$

$$\lambda = \frac{q^3 H^2 \Omega^2}{r^2 \mathcal{D}} \quad (28)$$

is a dimensionless eigenvalue, and N is the vertical buoyancy frequency in the disk. (The detailed form of f_2 is not illuminating.) Equation (26) does not satisfy the conditions of the Sturm–Liouville theorem, because f_1 is not of definite sign and both f_1 and f_2 vanish at $z = \pm H$. (We note in passing that the singular point where $\hat{\omega}^2 = N^2$ is

only an *apparent* singularity, since both linearly independent solutions are in fact regular there.) However, it can still be demonstrated that the eigenvalues $\{\lambda_j\}$ are real and the eigenfunctions $\{\tilde{u}_j\}$ orthogonal in the sense that

$$\int \rho \tilde{u}_j^* \tilde{u}_k dz = 0 \quad (29)$$

for any two modes with distinct eigenvalues. (Here and below, integrals are taken over the full vertical extent of the disk.) This is a limiting case of a more general orthogonality relation,

$$\int \rho (\tilde{u}_j^* \tilde{u}_k + \tilde{w}_j^* \tilde{w}_k) dz = 0, \quad (30)$$

which applies to the eigenfunctions away from resonances studied by KP. Moreover, it can be asserted that the eigenfunctions form a complete set on the space of continuous functions on $(-H, H)$, although, technically, the pointwise convergence of an eigenfunction expansion is non-uniform with respect to z at the end-points where the weight function ρ vanishes.

By rewriting equation (24) in the form

$$\Psi_m = \frac{r\mathcal{D}}{\pi\hat{\omega}} \sum_j \frac{s_j a_j}{q_j} \tilde{u}_j(z), \quad (31)$$

and using the orthogonality relation, we obtain the coefficients as

$$a_j = \frac{\pi\hat{\omega}s_j q_j \Psi_m}{r\mathcal{D}} \int \rho \tilde{u}_j^* dz \int \rho |\tilde{u}_j|^2 dz. \quad (32)$$

5. DERIVATION OF THE TORQUE FORMULA

We now proceed to show that the torque exerted by a companion object at a Lindblad resonance is precisely equal to the value derived under a two-dimensional approximation. The radial velocity perturbation corresponding to the collection of waves excited at the resonance is known from §4.2 to have an inner expansion

$$u(x, z) = \sum_j a_j \tilde{u}_j(z) [Ai(q_j x) + is_j Gi(q_j x)] \quad (33)$$

in the vicinity of the resonance, where $s_j = \pm 1$ is still to be determined, and a factor $\exp(-i\omega t + im\phi)$ is understood. From the asymptotic forms (Abramowitz & Stegun 1965)

$$x \rightarrow +\infty : Ai(x) \pm iGi(x) \sim \pm i\pi^{-1} x^{-1}, \quad (34)$$

$$x \rightarrow -\infty : Ai(x) \pm iGi(x) \sim \pm i\pi^{-1/2} (-x)^{-1/4} \times \exp \left\{ \mp i \left[\frac{2}{3} (-x)^{3/2} + \frac{1}{4} \pi \right] \right\}, \quad (35)$$

it is clear that the component of the solution labeled j matches on to a WKB traveling wave in the region $q_j x < 0$ and on to a decaying disturbance in the region $q_j x > 0$.

For single WKB waves of the disk it can be shown that the flux of angular momentum wave action, averaged over t , integrated over ϕ and z , and measured in the direction of increasing r , is

$$F^{(a)} = \frac{\pi r m}{k} \left(\frac{\hat{\omega}^2 - \kappa^2}{\hat{\omega}^2} \right) \int \rho |u|^2 dz. \quad (36)$$

The density of angular momentum wave action, similarly averaged and integrated, is

$$A^{(a)} = \frac{\pi r m}{\hat{\omega}} \int \rho (|u|^2 + |w|^2) dz, \quad (37)$$

and a straightforward application of first-order perturbation theory confirms that the ratio $F^{(a)}/A^{(a)}$ is equal to the radial group velocity

$$v_g = \frac{\partial \hat{\omega}}{\partial k} = \frac{(\hat{\omega}^2 - \kappa^2)}{\hat{\omega} k} \int \rho |u|^2 dz \Big/ \int \rho (|u|^2 + |w|^2) dz \quad (38)$$

which is the slope of the WKB dispersion relation. We therefore identify the direction of propagation of a WKB wave according to the sign of its radial group velocity.

Consider first the outer limit $x \rightarrow -\infty$ of equation (33) for a component with $q_j > 0$. The wavenumber, computed as the derivative of the phase, is

$$k \sim s_j q_j (-q_j x)^{1/2} r^{-1}. \quad (39)$$

It follows that

$$\text{sgn}(v_g) = s_j \text{sgn}(\mathcal{D}) \text{sgn}(\hat{\omega}), \quad (40)$$

and, since $\text{sgn}(\mathcal{D}) = -\text{sgn}(\hat{\omega})$ for a Keplerian disk (with the convention that $m > 0$), the outgoing wave that is required by causality is the one with $s_j = +1$. From equations (33), (35), and (36), the angular momentum flux associated with the wave is

$$F_j^{(a)} = \frac{r^2 m \mathcal{D} |a_j|^2}{\hat{\omega}^2 q_j^2} \int \rho |\tilde{u}_j|^2 dz, \quad (41)$$

although we emphasize that this is measured in the direction of increasing r , while the wave propagates into $r < r_L$. By a similar argument it can be shown that, for a component with $q_j < 0$, the required wave has $s_j = -1$ and carries an angular momentum flux

$$F_j^{(a)} = -\frac{r^2 m \mathcal{D} |a_j|^2}{\hat{\omega}^2 q_j^2} \int \rho |\tilde{u}_j|^2 dz \quad (42)$$

into $r > r_L$. From equation (32), the torque exerted on the disk is therefore

$$\begin{aligned} T &= -\frac{r^2 m \mathcal{D}}{\hat{\omega}^2} \sum_j \frac{|a_j|^2}{q_j^2} \int \rho |\tilde{u}_j|^2 dz \\ &= -\frac{\pi^2 m \Psi_m^2}{\mathcal{D}} \sum_j \left| \int \rho \tilde{u}_j dz \right|^2 \Big/ \int \rho |\tilde{u}_j|^2 dz \\ &= -\frac{\pi^2 m \Sigma_L \Psi_m^2}{\mathcal{D}}, \end{aligned} \quad (43)$$

where $\Sigma_L = \int \rho dz$ is the surface density at the resonance, and we have made use of the completeness of the eigenfunctions $\{\tilde{u}_j\}$. This formula is in precise agreement with equation (A10) of GT79. This result is not surprising since the 2D torque formula holds under a variety of physical conditions (Goldreich & Tremaine 1982; Papaloizou & Lin 1984). For non-Keplerian rotation curves, one cannot rule

out the possibility that $\text{sgn}(\mathcal{D}) = \text{sgn}(\hat{\omega})$, and so a more general formula is

$$T = -\text{sgn}(\hat{\omega}) \frac{\pi^2 m \Sigma_L \Psi_m^2}{|\mathcal{D}|}. \quad (44)$$

We now introduce a specific disk model which is used for all the numerical calculations in this paper. The disk is Keplerian and its vertical structure is polytropic, with index $s = 3$. The adiabatic exponent is taken to be $\gamma = 5/3$. For this model we have computed the fraction

$$f_j = \left| \int \rho \tilde{u}_j dz \right|^2 \Big/ \Sigma_L \int \rho |\tilde{u}_j|^2 dz \quad (45)$$

of the torque carried by each mode. The results for the f mode and the first three g and r modes are presented in Table 1, together with the corresponding eigenvalues λ_j (defined by eq. [28]). It is clear that almost all the angular momentum is transported by the f mode, although the r and g modes are also weakly excited. These first seven modes together account for 99.93% of the torque. For obvious reasons we focus on the propagation of the f mode for the remainder of this paper. However, it is worth noting that the r modes propagate away from the resonance in the opposite direction to the f and g modes. The results in Table 1 are independent of m .

6. PROPAGATION OF MODES IN A KEPLERIAN DISK

6.1. Basic properties of the f mode

In this section, we summarize the properties of the single most important mode in this problem, the f^e mode or fundamental mode of even symmetry. The eigenfunction of this mode, whether at the resonance or away from it, is uniquely characterized as follows. The pressure perturbation (or radial velocity perturbation) has no nodes in $-H < z < H$. The vertical velocity perturbation has only a single node at $z = 0$, as required by symmetry. This form of the eigenfunction allows a large overlap integral with the forcing potential which is independent of z , and explains why this mode is excited more than any other (see eq. [32]).

The dispersion relation for this mode in our model disk (which is Keplerian and polytropic, with $s = 3$ and $\gamma = 5/3$) is shown in Figure 2a. Also shown is the asymptotic form

$$\hat{\omega}^2 \sim \Omega^2 k H \quad (46)$$

derived by Ogilvie (1998), which is valid in the limit $kH \rightarrow \infty$. Since the surface gravity of the disk is $g_s = \Omega^2 H$, the above equation is consistent with the well-known dispersion relation for surface waves in a deep layer of water. A more accurate approximation, which takes into account the effects of rotation and stratification, is

$$\hat{\omega}^2 \sim \Omega^2 k H + \frac{1}{2} \kappa^2 - \frac{1}{2} s \Omega^2, \quad (47)$$

and this is shown in Figure 2b to provide an excellent approximation even for values of kH as small as 3.

The form of the eigenfunction in this limit also corresponds to that expected of a surface gravity mode. For definiteness, we describe a wave traveling radially outwards in the disk, but inward traveling waves and standing waves are very similar in form. The wave is trapped in a layer of

TABLE 1
MODES EXCITED AT A LINDBLAD RESONANCE.

Mode	λ_j	f_j
f	6.16	0.9678
g_1	112.26	0.0010
g_2	236.47	0.0003
g_3	401.73	0.0002
...
r_1	-18.98	0.0277
r_2	-98.32	0.0018
r_3	-237.42	0.0005
...

characteristic thickness k^{-1} near the surface of the disk, and in this layer the asymptotic forms

$$u \sim A \cos(kr - \omega t + m\phi) \exp(-k\delta), \quad (48)$$

$$w \sim A \sin(kr - \omega t + m\phi) \exp(-k\delta) \quad (49)$$

are valid, where $\delta = H - |z|$. This velocity field is both irrotational and solenoidal (i.e. non-compressive). The azimuthal velocity is smaller by a factor $O((kH)^{-1/2})$. In this limit, the even and odd f modes are indistinguishable since there is a loss of contact between the two surfaces of the disk (KP).

For small values of kH , the mode departs from the behavior described above. An approximation valid in the limit $kH \rightarrow 0$ is

$$\hat{\omega}^2 \sim \kappa^2 + k^2 H^2 \Omega^2 / \lambda, \quad (50)$$

where $\lambda > 0$ is the dimensionless f-mode eigenvalue defined by equation (28). This form is reminiscent of the dispersion relation $\hat{\omega}^2 = \kappa^2 + c_s^2 k^2$ for the two-dimensional mode in an isothermal disk (LP). While it is true that λ depends on γ , implying that the f^e mode is partly compressive in this limit, nevertheless λ has a non-trivial limit when $\gamma \rightarrow \infty$. Therefore the mode behaves partly compressively near the resonance, but only when the disk is compressible. The mode does not disappear in the incompressible limit.

We emphasize how this description differs from earlier, less accurate theories of waves in disks. If the disk is described as a two-dimensional fluid, then all radially propagating modes are inherently compressive by virtue of the constraints on the fluid, and would normally be described as sound waves modified by rotation. In a three-dimensional disk, a two-dimensional mode of this form exists only if the disk is vertically isothermal. In general, however, the principal mode excited at an LR in a three-dimensional disk is the f^e mode, which is not inherently compressive. Moreover, this mode cannot be described using a vertical WKB approximation (cf. Vishniac & Diamond 1989; Goodman 1993) because it has no pressure nodes in the vertical direction, being, if anything, evanescent rather than wavelike.

6.2. Propagation and damping of the f mode

6.2.1. Remarks on the nonlinear development of the f mode

If the waves excited at a resonance were able to propagate radially without dissipation, they would reflect from the radial boundaries and establish a standing wave pattern. The net transfer of angular momentum and energy between the disk and the companion would then be zero. In order for the waves to have a significant dynamical effect on the evolution of the system, they must deposit their angular momentum (either positive or negative) in the disk as a result of being damped. This can happen within linear theory if there is sufficient viscosity, but otherwise nonlinear dissipation is required. As noted by KP, the concentration of modes near the surface of a polytropic disk is likely to result in enhanced dissipation through the formation of shocks.

It might be argued that, since the f mode is approximately non-compressive, it would form shocks less easily and would therefore be less susceptible to this type of dissipation. However, little is known about the nonlinear development of surface gravity modes in a compressible fluid. In the case of an incompressible fluid, it is well known that when the amplitude of a surface gravity wave is increased, the distorted profile of the surface changes from a sinusoidal shape to one with sharper crests, forming an angle approaching 120° . This happens when the velocity perturbation is comparable to the phase velocity $(g_s/k)^{1/2}$ (e.g. Stokes 1880; Lamb 1932), and causes the crests to break. Although we consider it more probable that the nonlinear development in a compressible fluid will lead to shocks rather than breaking crests, it is still appropriate to normalize the solution described by equations (48) and (49) according to

$$u \sim \mathcal{N} \left(\frac{\Omega^2 H}{k} \right)^{1/2} \cos(kr - \omega t + m\phi) \exp(-k\delta), \quad (51)$$

where \mathcal{N} is a measure of the nonlinearity of the wave. Indeed, when this is substituted into the nonlinear equations, it can be seen that the nonlinear terms become comparable to the linear ones when $|\mathcal{N}| \exp(-k\delta) \approx 1$. Therefore the wave can be considered to be marginally nonlinear at

the surface when $|\mathcal{N}| \approx 1$, but, when $|\mathcal{N}| \approx e$, say, a substantial fraction of the wave action can be considered to be subject to nonlinearity.

6.2.2. Approximate, analytical treatment of radial propagation

To be specific, we now consider the case of objects in a circular orbit. (The results for non-circular orbits that provide eccentric LRs do not differ in a substantial way from the analysis in this and the following subsection.) There is a Keplerian disk in which the angular velocity is

$$\Omega = \left(\frac{GM}{r^3} \right)^{1/2} = \Omega_c \left(\frac{r}{r_c} \right)^{-3/2}, \quad (52)$$

where r_c and Ω_c are the radius and angular velocity, respectively, of the corotation radius. The dimensionless intrinsic frequency of a mode with angular pattern speed Ω_c is

$$\frac{\hat{\omega}}{\Omega} = m \left[\left(\frac{r}{r_c} \right)^{3/2} - 1 \right], \quad (53)$$

and the radii of the LRs are

$$r_L = \left(\frac{m \mp 1}{m} \right)^{2/3} r_c, \quad (54)$$

where the upper and lower signs refer to the ILR and OLR, respectively. By combining equation (53) with the dimensionless dispersion relation (Figure 2), we can derive the variation of the dimensionless wavenumber kH with r/r_c . The results for various values of m are shown in Figure 3. It is clear that, after the wave has propagated over a radial distance comparable to r_L/m from the resonance, kH has become sufficiently large that the wave can be described accurately as a surface gravity mode. This makes it possible to determine the amplitude of the wave analytically.

Let f denote the fraction of the torque carried by the f^e mode. Then, from equation (36), the flux of angular momentum wave action associated with the wave is

$$\frac{\pi r m}{k} \left(\frac{\hat{\omega}^2 - \Omega^2}{\hat{\omega}^2} \right) \int \rho |u|^2 dz = \mp f T. \quad (55)$$

In the limit in which the wave can be described as a surface gravity mode, kH can be approximated as $\hat{\omega}^2/\Omega^2$, which itself can be considered large compared to unity, while the above integral becomes

$$\begin{aligned} \int \rho |u|^2 dz &\approx 2\rho_0 \mathcal{N}^2 \left(\frac{\Omega^2 H}{k} \right) \int_0^\infty \left(\frac{2\delta}{H} \right)^s e^{-2k\delta} d\delta \\ &= \Gamma(s+1) \mathcal{N}^2 (kH)^{-s} \left(\frac{\rho_0 \Omega^2 H}{k^2} \right). \end{aligned} \quad (56)$$

If we assume that $H \propto r$ and $\rho_0 \propto r^{-p}$, the approximate radial variation of \mathcal{N} is given by

$$\mathcal{N}^2 \propto \left[\left(\frac{r}{r_c} \right)^{3/2} - 1 \right]^{2(s+3)} \left(\frac{r}{r_c} \right)^{p-2}. \quad (57)$$

As the wave approaches the radial center of the disk, $\mathcal{N}^2 \propto r^{p-2}$. It is quite plausible that $p > 2$ (implying that

the surface density increases inwards faster than r^{-1}), in which case the wave becomes *less* nonlinear as it travels inwards. Otherwise, if the surface density increases inwards less rapidly, \mathcal{N}^2 increases inwards no faster than r^{-1} . For many cases of interest, there is therefore nothing singular about the wave approaching the radial center of the disk.

As the wave propagates outwards into $r \gg r_c$, $\mathcal{N}^2 \propto r^{p+3s+7}$. This means that, for any reasonable density profile and polytropic index, the wave is very likely to become nonlinear as it propagates outwards.

6.3. Numerical results

We have computed numerically the radial propagation of the f^e mode in a Keplerian disk using the method outlined in the analytical treatment above, except that we do not apply the limiting analytic forms for surface gravity waves described after equation (55). The model disk has the standard parameters $s = 3$, $\gamma = 5/3$, and also $H \propto r$ and $\rho_0 \propto r^{-2}$. The results are presented as color images in Plates 1 and 2, for the cases $m = 2$ and $m = 10$, respectively. In each case, panels (a) and (b) refer to the inward propagation from the ILR, with radii $0 < r < r_L$ shown. Panels (c) and (d) refer to the outward propagation from the OLR, with radii $r_L < r < 2r_L$ shown. In order to show the detail clearly, the vertical scale is greatly exaggerated. The two quantities plotted are the density of angular momentum wave action, averaged over time,

$$\mathcal{A}^{(a)} = \left(\frac{m}{2\hat{\omega}} \right) \rho (|u|^2 + |w|^2), \quad (58)$$

and the RMS velocity perturbation,

$$u_{\text{RMS}} = \left[\frac{1}{2} (|u|^2 + |v|^2 + |w|^2) \right]^{1/2}. \quad (59)$$

In panels (a) and (c), we plot the logarithm (to the base 10) of $|\mathcal{A}^{(a)}|$, in units of $|T| \Omega_L^{-1} r_L^{-1} H_L^{-2}$. In panels (b) and (d), we plot the logarithm of $u_{\text{RMS}}/(\Omega H)$, in units of $|T|^{1/2} \Sigma_L^{-1/2} r_L^{-1/2} H_L^{-3/2} \Omega_L^{-1}$. The former quantity shows how the activity of the wave is distributed, in both the vertical and the radial directions. The latter quantity, apart from a normalization factor, is intended as a measure of the velocity amplitude of the wave relative to the local sound speed at the mid-plane. It is a more conservative measure of nonlinearity than \mathcal{N}^2 , and may be more appropriate in regions close to the resonance, where the f^e mode behaves partly compressibly and may produce shocks more easily.

If the disk extends continuously over the resonance, the torque can be calculated in terms of the standard formula, equation (43). In many cases of interest, however, the LR truncates the disk. In such cases, the disk edge partially overlaps with the resonance and the torque is often physically determined by the viscosity. The density at the resonance then adjusts so that its average value over the resonance width provides the needed torque in accordance with equation (43). The meaning of Σ_L in the normalization of the velocity is the surface density expected on the basis of the smooth power-law density profile in the main body of the disk, rather than its actual value near the LR. In the case of a disk with an edge, the results in Plates 1 and 2 apply where the power-law density distribution holds in the disk.

Some care is required in interpreting Plates 1 and 2. They are plotted as if H/r were equal to 1/2 (for the ILR) or 1/4 (for the OLR), but this is done to allow a convenient visualization and has no intrinsic significance. The value of H/r is immaterial provided only that it is small; indeed the results become more accurate as $H/r \rightarrow 0$. The channeling of the wave occurs on a radial scale that is independent of H . There is a region of characteristic width $(H^2 r)^{1/3}$ around the resonance where, properly, the Airy functions should be used, but no attempt has been made to include this on the plots because it would require a definite choice to be made for the value of H/r . In fact, the singularity of the WKB solutions at the resonance is barely evident on the plots.

For the case $m = 2$ (Plate 1), the inward propagation leads to a mild concentration of the wave action near the surfaces of the disk. However, the amplitude of the wave near the surface does not increase by large amounts away from the resonance and in fact tends to a constant value as the radial center of the disk is approached, in accordance with equation (57). The (dimensionless) amplitude increases by about a factor of 5 from the neighborhood of the LR to the disk center. With a larger value of p (more rapid density increase toward the center), the overall amplitude increase would be less and the amplitude would decrease near the center. By contrast, a much more significant channeling effect occurs in the outward propagation, and the amplitude near the surface increases strongly away from the resonance, also in accordance with equation (57).

For the case $m = 10$ (Plate 2), the channeling effect is very pronounced for both inward and outward propagation. In the regions close to the resonances, there is an approximate symmetry between the two cases. However, it is again seen that the amplitude tends to a (large) constant value as $r \rightarrow 0$ in the inward propagation, while the amplitude increases strongly as $r \rightarrow \infty$ in the outward propagation.

7. APPLICATION TO BINARY AND PROTOPLANETARY SYSTEMS

In this section, we explore the consequences of this work for some astrophysical situations. In any binary star system, up to three disks can occur. There may be two circumstellar (CS) disks, each of which orbits about one of the stars. In addition, there may be a circumbinary (CB) disk that orbits around the entire system. Powerful tidal forces present in binary systems clear large gaps in the disks, of order a few times the binary semi-major axis (Lin & Papaloizou 1993; Artymowicz & Lubow 1994, hereafter AL), which separate the disks from each other. As a consequence of the large size of the gaps, the disks experience tidal forcing primarily from relatively low azimuthal wavenumbers $m \sim 2$.

As discussed in the Introduction, there are several dissipation mechanisms that can act to damp the waves. This section contains some discussion of turbulent viscous dissipation of waves. The nature of the disk turbulence is quite uncertain. Additionally, the interaction of the f mode with turbulence is complicated by the fact that the largest turbulent eddies carry most of the viscosity, but they may not interact efficiently to damp the waves. Some simple-minded arguments suggest that the spatial damping rate in the radial direction is $k_I \sim \alpha k (k \bar{H})^b$, where α is the

usual parameterization of viscosity and b is a number of small absolute value that depends on the details of the turbulence. Such complications add to the uncertainty in k_I , but we adopt $k_I \sim \alpha k$ as a plausible estimate.

In general, we expect wave channeling to amplify the wave substantially over a radial length scale r_L/m for which $kH \gtrsim 1$. A rough relative measure of the importance of turbulent wave damping to wave channeling is $k_I r_L/m \sim \alpha r_L/(mH)$. For protostellar or protoplanetary disks, this ratio is less than unity, while for CV disks it is greater than unity, as is discussed below.

One important example of CB disks occurs in young binary stars, where the remnant material involved in the star-formation process orbits around the binary. Typically these binaries have eccentricities $e \sim 0.3$ and the LRs are associated with the eccentric motions of the system (AL). An LR torque is responsible for truncating the CB disk at its inner edge. Such CB disks have been inferred to exist from the spectral energy distribution of some young binaries (Mathieu 1994). Based on our results in Plate 1, we expect that significant wave channeling would occur in a thermally stratified CB disk within a distance $\sim r_L/2$ from the resonance. We expect that strong nonlinear wave damping would occur in a CB disk, but exactly where this would occur depends on the level of nonlinearity of the wave near the LR. The 2D simulations of CB disks using smoothed-particle hydrodynamics (SPH) show that the wave is somewhat nonlinear near resonance, as is apparent from the prominence of the spiral arms near the disk's inner edge (AL). This effect provides some justification for the assumption that the wave damping occurs relatively close to the resonance (as occurs in 2D SPH simulations of CB disks, but possibly due to artificial viscosity).

In the case of CS disks in young (eccentric) binary systems, the eccentric Lindblad resonances can be important (GT80; AL). As seen in Plate 1, the wave channeling effect is relatively weak, but of possible importance as the level of wave nonlinearity increases by about a factor of 5 to the disk center. For low amplitude waves in the outer parts of the disk, the wave may well survive to the center of the disk, provided that other damping effects can be neglected. If the wave reflects off the central star, then the process of wave generation can become reversible, as the reflected wave returns to the LR. The net effect is a zero LR torque. Other wave damping effects, such as viscous wave damping or damping within the star, may play a role in preventing reversibility.

In protostellar disks, the value of α has been estimated to be of order 10^{-2} (e.g. Hartmann et al. 1998). The extent of the turbulent decay of a wave over radius comparable to r_L can be estimated by taking $kH \sim m^2$, $H/r \sim 0.1$, and $m \simeq 2$ for binary star forcing. The wave amplitude decays by roughly a factor $\exp(-k_I r_L) \sim 0.7$. This plausibly provides some damping in a protostellar CS disk. For a CB disk, nonlinear damping by wave channeling will likely dominate, if the wave is slightly nonlinear near resonance.

In addition, several classes of mass-transfer binaries (e.g. X-ray binaries and CVs) possess CS disks. These close binaries have nearly zero eccentricity, as a consequence of the tidal interactions between the system objects. Under these conditions, there are no eccentric LRs and the disk is sufficiently truncated that no (non-eccentric) LRs can

lie within the the disk. However, the closest LR, corresponding to $m = 2$, is sufficiently powerful to generate waves off-resonance as a result of the non-zero width of the resonance (see, e.g., Savonije, Papaloizou, & Lin 1994). Again, our results suggest that wave channeling is of possible importance, but is not very powerful. In practice, the vertical resonances may play a more important role in such systems, since these resonances can lie within the disk (Lubow 1981).

CV disks surround white dwarf stars and the value of α has been estimated to be of order 0.1 during outbursts, but could be much lower during quiescence (e.g. Cannizzo 1993). The extent of turbulent radial decay rate over radius comparable to r_L can be estimated by taking $kH \sim m^2$, $H/r \sim 0.02$, and $m \simeq 2$ for binary star forcing. The wave amplitude radial decay over a radius is of order 10^8 . These estimates are crude, but suggest that the turbulent wave attenuation is severe (at least during outbursts), more severe than wave channeling, and would damp the f mode.

In protoplanetary disks, the planets carve out relatively small gaps or possibly no gap at all. As a result, several high- m LRs can lie within the disk. Under such conditions, it has been shown that the dominant torque comes from the LR having $m \approx r/H$ (GT80; Ward 1986, 1988; Artymowicz 1993a,b). For typical protoplanetary disks, we then expect $m \sim 10-20$ to be most important. Our calculations have assumed that $m \ll r/H$, so that we cannot apply our analysis throughout the resonant region. In addition, these LRs have a vertical forcing contribution that is comparable to the horizontal forcing, and both of these vary somewhat with z (Ward 1988; Artymowicz 1993a). The present analysis assumed vertically constant horizontal forcing and ignored some azimuthal terms in the dynamical equations, as discussed in §3.2. In principle, our methods could be extended to handle these complications.

However, even in this case, some important conclusions can be drawn from the analysis in this paper. The region of resonant forcing in this case can be shown to be of order H in both the radial and vertical directions (rather than $(H^2r)^{1/3}$ for the radial and H for the vertical directions in the case $m \ll r/H$). Furthermore, it can be shown that the waves for which $m \approx r/H$ do approximately satisfy the equations of this paper at distances of order a few times H from the LR. This is because the radial wavenumber increases so rapidly with increasing distance from resonance that it quickly dominates the azimuthal wavenumber and makes our approximations valid. The f mode suffers wave channeling at radial distances from the resonance of order $r_L/m \sim H$ in this case.

Therefore, we are led to the simple picture that the f mode is launched in protoplanetary disks from a region of size of order H . It undergoes wave channeling on a similar scale of a few H . As can be seen from Plate 2 for $m = 10$ (which we argue is approximately valid at distances greater than about $r_L/5$ from r_L for $H/r \sim 0.1$), strong nonlinear damping can then occur with increasing distance from the LR.

We expect that a full 3D analysis of the resonant region would reveal that the f mode is still strongly excited in protoplanetary disks, compared with other modes. The reason is that the vertical component of the tidal forcing is

not dominant and has a single zero at mid-plane. Furthermore, the vertical variation of the horizontal forcing within the disk is not large, especially when the density weighting is taken into account (Ward 1986; Artymowicz 1993a). So the tidal forcing should preferentially drive modes with no or few vertical nodes. In any case, the g and r modes that are excited at an LR undergo wave channeling that is at least as strong as that of the f mode.

In the case of young Jupiter in the solar nebula, GT80 estimated that the wave-induced velocities are already mildly nonlinear (having Mach number about 0.3) at the LR. We therefore expect that shock damping would be important of a scale of order H from resonance, where wave channeling would occur. The extent of turbulent wave damping on that scale can be estimated by taking $k \sim H^{-1}$ and $\alpha \sim 0.01$. We then obtain the level of turbulent damping $k_1 H \sim 0.1$, and so we therefore expect that wave channeling strongly limits giant planet driven wave propagation in thermally stratified disks.

8. SUMMARY AND DISCUSSION

8.1. Summary of results

We have analyzed the 3D response to tidal forcing of a gaseous disk having a vertical temperature variation. The unperturbed vertical disk structure was modeled as locally polytropic. We have considered effects at Lindblad resonances (LRs), subject to the thin disk approximation $H \ll r/m$, for which the LRs provide horizontal forcing that is independent of height. In the standard vertically isothermal case considered to date, the horizontally propagating 2D mode (sound wave) carries all the resonantly generated angular momentum, but only if the thermodynamic response of the disk is also isothermal.

In the vertically polytropic case, the f mode has a role equivalent to that of the 2D mode, although r and g modes are also launched at LRs (see Figure 1). The mode launched at vertical resonances (Lubow 1981) can be shown to be the p_1^e mode. We have found that nearly all the torque exerted at an LR is carried by the f mode (see Table 1). Near resonance, the f mode behaves in a similar manner to the 2D mode in the isothermal case, in that it occupies the full vertical extent of the disk and behaves somewhat compressibly. The f mode is almost two-dimensional near resonance in that the vertical velocities are smaller than the horizontal by a factor of order $(H/r)^{1/3}$. However, away from resonance, the behaviors of the f and 2D modes differ radically (see §6.2). At a distance $\sim r_L/m$ from the resonance, the f mode begins to concentrate its energy near the surface of the disk, a process which we have called wave channeling. In this regime, the f mode behaves like a surface gravity mode (see Plates 1 and 2). In most cases, the wave amplitude increases by many orders of magnitude with distance from resonance, so that it is very likely that shocks will develop which would damp the wave. An important exception to this last statement occurs for the $m = 2$ ILR. The wave generated there undergoes relatively mild wave channeling and consequently a relatively mild increase in nonlinearity (by about a factor of 5). The amount of increase depends on the density distribution in the disk and could even result in a decrease in dimensionless amplitude near the disk center. Dissipation by turbulent viscosity is likely impor-

tant in some cases, such as CV disks. On the other hand, the wave generated at the $m = 2$ OLR does exhibit strong wave channeling. These results indicate that circumbinary disks, as found around young binaries, and protoplanetary disks perturbed by planets, are subject to strong effects of wave channeling (see §7).

8.2. Discussion

The results in this paper differ from the previously accepted picture for wave propagation in thermally stratified disks (e.g. LPS). The standard expectation was that a wave launched at a Lindblad resonance would begin propagating horizontally, but the wavefront would be rapidly refracted upwards as a result of the decrease in sound speed with increasing height above the mid-plane. After advancing a distance comparable to the disk thickness H , the wavefront would be substantially tilted upwards. The wave would then propagate vertically into the atmosphere of the disk, where it would shock. This model is based on the idea that the launched wave is a pressure wave or p mode in a high-frequency acoustic limit, so that one can consider the wavefront to propagate at the local sound speed without being affected by inertial or buoyancy forces.

Our results provide a different picture. We have found that the wave cannot be considered to propagate vertically, since it is in fact a vertically evanescent f mode. In this view, taken in LP and KP, the disk behaves like a waveguide in which the wave is vertically confined. However, somewhat similar to the standard picture, the wave energy does rise to the surface of the disk as the wave propagates away from the resonance. But this wave channeling process is effective over a distance of order r_L/m , where r_L is the radius of the Lindblad resonance and m is the azimuthal wavenumber. It does not depend on the disk thickness, provided that $H/r \ll 1$.

This can be understood roughly as follows. The wave channeling occurs because of the radial variation of the dimensionless intrinsic frequency of the wave, $(\omega - m\Omega)/\Omega$. This is equal to $\pm\kappa/\Omega$ at the Lindblad resonance, but increases rapidly in magnitude over a distance of order r_L/m . The wave therefore proceeds rapidly along the f-mode branch of the dispersion relation. In the high-frequency limit, as described in §6.1, the mode behaves like a surface gravity wave and is confined near the surface of the disk. (This would be true even in an incompressible disk in which refraction cannot operate.) The surface-gravity-mode dispersion relation is approximately $(\omega - m\Omega)^2 \approx g_s k$, where the surface gravity $g_s = \Omega^2 H$ and k is the radial wavenumber. It can be seen (see §6.1) that the mode is confined to the disk surface in a layer of vertical thickness $\delta \sim k^{-1}$. It then follows from the dispersion relation that $(\omega - m\Omega)^2/\Omega^2 \sim H/\delta$. As a result, the wave becomes confined (channeled) near the disk surface (i.e., $\delta/H \lesssim 1/2$) over a radial distance from resonance of order r_L/m .

Another issue concerns the boundary conditions. In LPS, the anticipated shocks in the disk atmosphere were represented in their simulation by an upper boundary condition that included some amount of dissipation. In our analysis of a polytropic disk, we have applied a bound-

ary condition at the disk surface that acts to reflect waves rather than absorb energy. Even in a purely isothermal disk without a definite surface, as demonstrated by LP, all the modes are confined vertically and do not propagate vertically to infinity. This is a consequence of the increase in vertical gravity with height.

Our treatment of the boundary is valid in the limit of high optical depth, where the atmosphere occupies a negligible mass. In particular, the effects of atmosphere are not strongly felt by the wave until $kH_{\text{atmos}} > 1$, with H_{atmos} being the density scale height at the base of the atmosphere. For a highly optically thick disk, H is much greater than H_{atmos} , and so $kH \gg 1$. When this condition occurs, the wave has been strongly channeled before much wave energy enters the atmosphere. We plan to extend our current analysis to include the effects of a disk atmosphere in a future paper.

The asymmetry in wave properties between the inner and outer LRs is most pronounced for low- m cases. For fixed m , the level of nonlinearity for ILR waves is lower than for OLR waves (see §6.2.2). One reason is that the density increases as the ILR wave propagates inward, while the density decreases as the OLR wave propagates outwards (see eq. [57]). The other cause of the asymmetry is that the f-mode dispersion relation is followed to higher wavenumbers in the exterior of the OLR than in the interior of the ILR, for low m (see Figure 3). Away from the LR, the f mode is vertically confined to a surface layer of thickness $\sim k^{-1}$. Due to wave action conservation, the confinement acts to increase the wave amplitude, causing substantial asymmetry in the case $m = 2$. In the high- m case, the behavior of the wavenumber becomes similar near the inner and outer LRs, and consequently the nonlinearity becomes important at comparable distances from the respective resonances.

A variant on the vertically polytropic model occurs for layered disks (Gammie 1996). In this model, some regions of protostellar or protoplanetary disks have turbulence restricted to the upper layers of the disk. The resulting vertical temperature structure is isothermal in the non-turbulent layer near mid-plane and the temperature declines with height in the outer turbulent layers. A wave launched from an LR in such a disk would probably require a longer distance from resonance to undergo wave channeling.

Given the large increases in wave velocities associated with wave channeling (see Plates 1 and 2), we expect that nonlinearities will cause the waves to shock and deposit angular momentum preferentially near the surface of the disk. We have described where nonlinearities are expected to become important in §6.2, based on a quasilinear estimate. Little work has been carried out to investigate the nonlinear behavior of f modes or surface gravity waves in a compressible fluid. It would be useful to conduct nonlinear simulations of the waves in such a disk.

We gratefully acknowledge support from NASA Origins of Solar Systems Grant NAGW-4156 and NATO travel grant CRG940189. We thank Jim Pringle for many discussions on this problem.

REFERENCES

Abramowitz, M., & Stegun, I. A. 1965, Handbook of Mathematical Functions (New York: Dover)

Artymowicz, P. 1993a, ApJ, 419, 155

Artymowicz, P. 1993b, ApJ, 419, 166

Artymowicz, P., & Lubow, S. H. 1994, ApJ, 421, 651 (AL)

Cannizzo, J.K. 1993, Theory of Accretion Disks 2, eds. Meyer, Duschl, Frank, NATO ASI series, p. 125.

Cassen, P., & Woolum, D. S. 1996, ApJ, 472, 789

Cox, J. P. 1980, Theory of Stellar Pulsation (Princeton: Princeton Univ. Press)

Gammie, C. F. 1996, ApJ, 457, 355

Goldreich, P., & Tremaine, S. 1979, ApJ, 233, 857 (GT79)

Goldreich, P., & Tremaine, S. 1980, ApJ, 241, 425 (GT80)

Goldreich, P., & Tremaine, S. 1980, ARA&A, 20, 249

Goodman, J. 1993, ApJ, 406, 596

Hartmann, L., Clavet, N., Gullbring, E., D'Alessio, P. 1998, ApJ, 495, 385

Korycansky, D. G., & Pringle, J. E. 1995, MNRAS, 272, 618 (KP)

Lamb, H. 1932, Hydrodynamics, 6th edn (Cambridge: Cambridge Univ. Press)

Lin, D. N. C., Papaloizou, J. C. B., & Savonije, G. J. 1990a, ApJ, 364, 326 (LPS)

Lin, D. N. C., Papaloizou, J. C. B., & Savonije, G. J. 1990b, ApJ, 365, 748

Lin, D. N. C., & Papaloizou, J. C. B. 1993, in Protostars and Planets III, ed. E. H. Levy & J. I. Lunine (Tucson: Univ. of Arizona Press), 749

Lubow, S. H. 1981, ApJ, 245, 274

Lubow, S. H., & Artymowicz, P. 1996, in Evolutionary Processes in Binary Stars, ed. R. A. M. J. Wijers, M. B. Davies, & C. A. Tout (Dordrecht: Kluwer), 53

Lubow, S. H., & Pringle, J. E. 1993, ApJ, 409, 360 (LP)

Mathieu, R. D. 1994, ARA&A, 32, 465

Ogilvie, G. I. 1998, MNRAS, in press

Papaloizou, J. C. B., & Lin, D. N. C. 1984, ApJ, 285, 818 ApJ, 463, L326

Savonije, G. J., Papaloizou, J. C. B., & Lin, D. N. C. 1994, MNRAS, 268, 13

Shu, F. H., Yuan, C., & Lissauer, J. J. 1985, ApJ, 291, 356

Stokes, G. G. 1880, in Mathematical & Physical Papers, Vol. 1 (Cambridge: Cambridge Univ. Press), 197

van Dyke, M. 1975, Perturbation Methods in Fluid Mechanics (Stanford: Parabolic Press)

Vishniac, E. T., & Diamond, P. 1989, ApJ, 347, 435

Ward, W. 1986, Icarus, 67, 164

Ward, W. 1988, Icarus, 73, 330

Yuan, C., & Cassen, P. 1994, ApJ, 437, 338

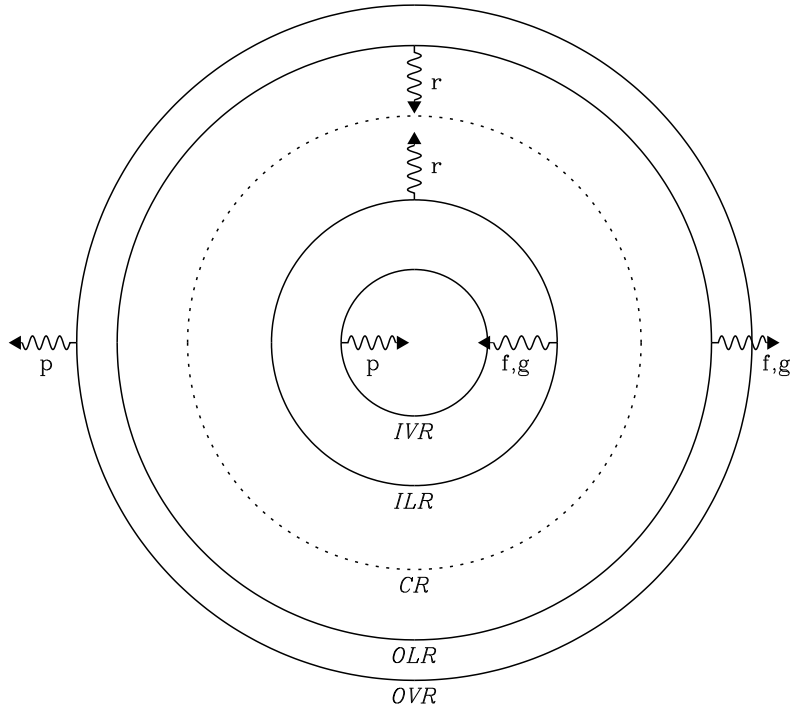


FIG. 1.— Propagation of non-axisymmetric waves in a Keplerian disk. The five radii marked are the corotation radius ('CR'), the inner and outer Lindblad radii ('ILR', 'OLR'), and the inner and outer (vertical) resonances of the first p mode of even symmetry ('IVR', 'OVR'). The diagram indicates where the different classes of modes are excited and where they propagate. (The parameters used here are $m = 2$, $s = 3$, and $\gamma = 5/3$.)

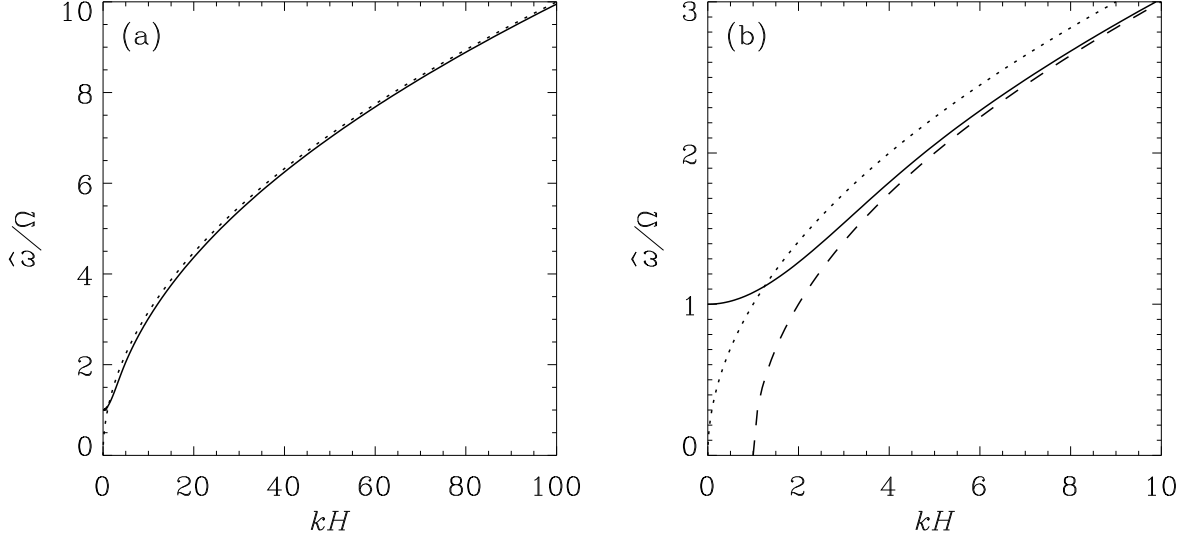


FIG. 2.—*Panel a:* dispersion relation (solid line) for the f^e mode in a Keplerian, polytropic disk with $s = 3$ and $\gamma = 5/3$. Also shown (dotted line) is the asymptotic form given in equation (46). *Panel b:* expanded view of the same dispersion relation (solid line). Also shown are the approximations given in equations (46) (dotted line) and (47) (dashed line).

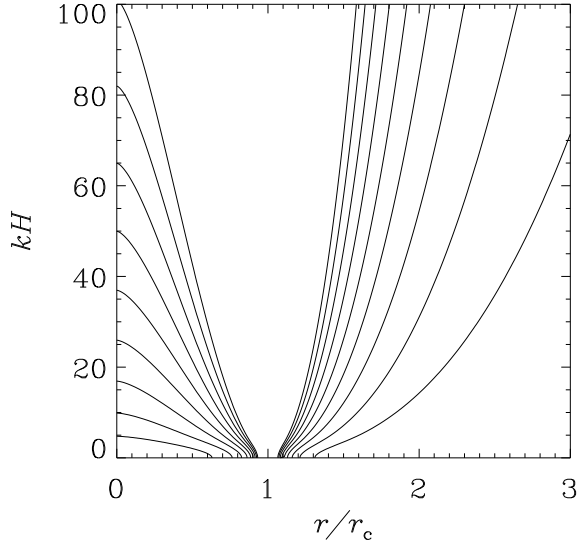


FIG. 3.—Variation of the dimensionless radial wavenumber with radius for the f^e mode in a Keplerian, polytropic disk with $s = 3$ and $\gamma = 5/3$. The nine curves plotted correspond to $m = 2, 3, \dots, 10$, from bottom to top.

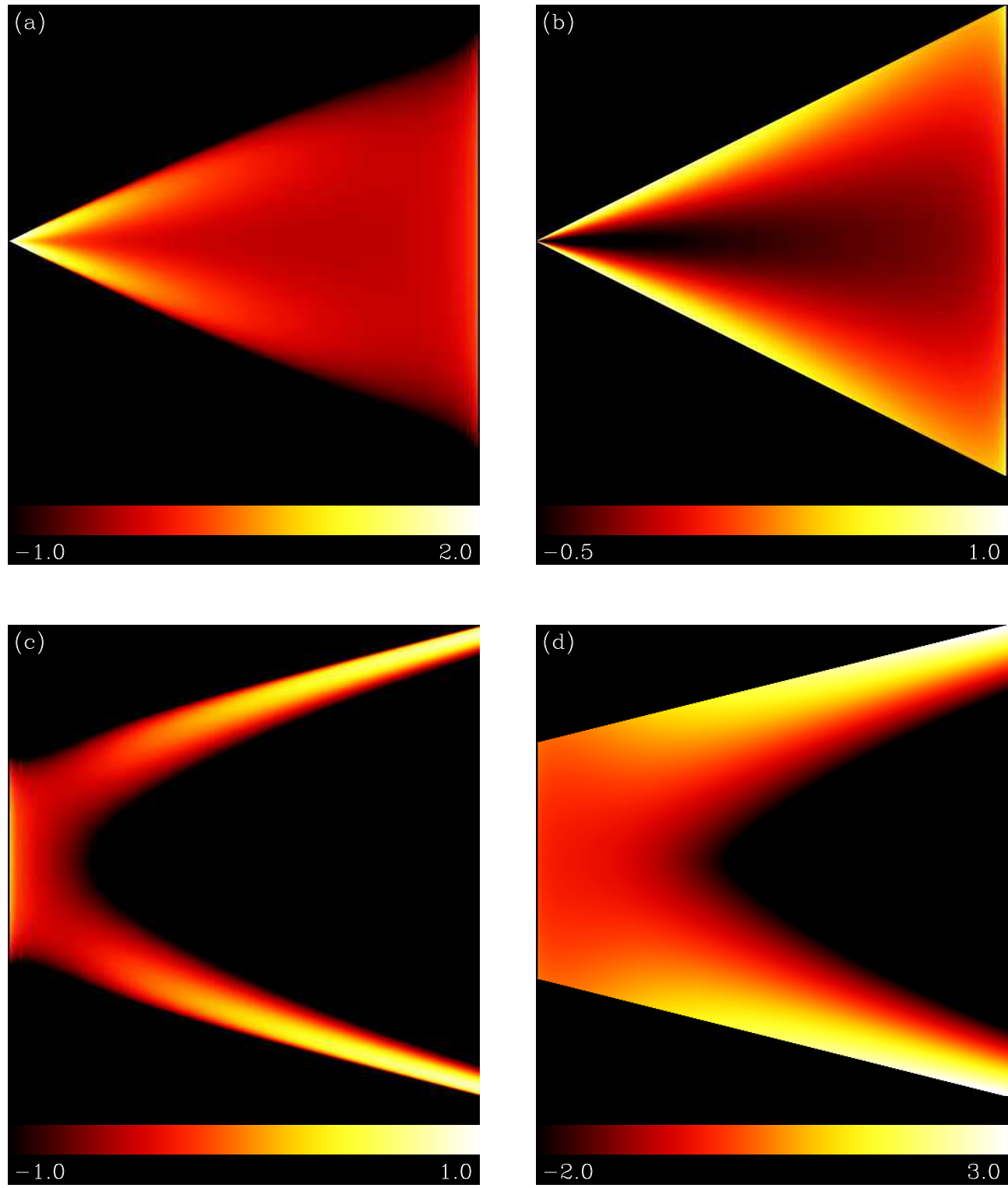


PLATE 1. (See Section 6.3 for discussion.)

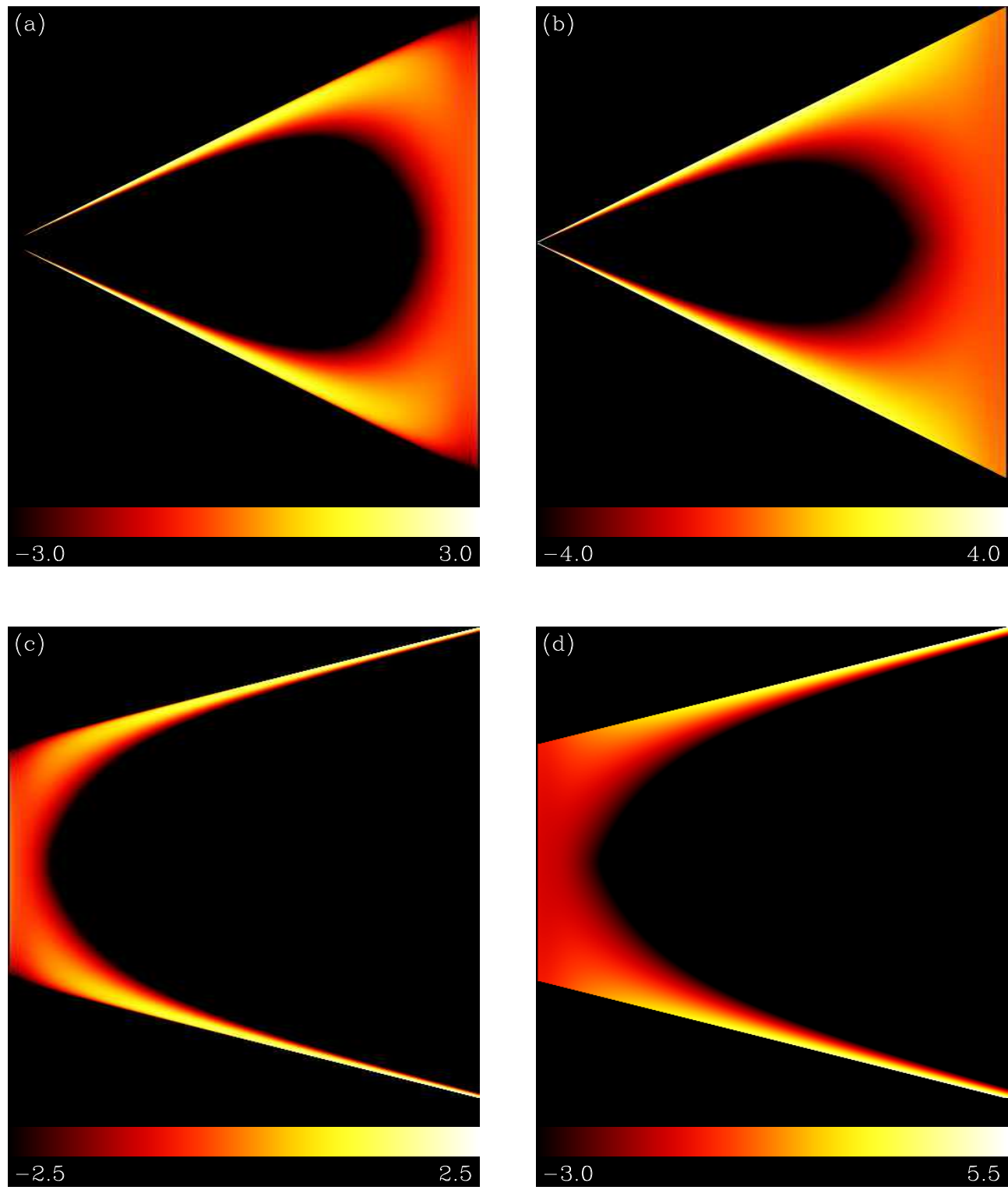


PLATE 2. (See Section 6.3 for discussion.)